

UKAEA-CCFE-PR(18)51

Vasili Kiptily, F. Belli, J. Eriksson, C. Hellesen,  
V.Goloborod'ko, K.Schöpf

# **On a fusion born triton effect in JET deuterium discharges with H- minority ICRF heating**

Enquiries about copyright and reproduction should in the first instance be addressed to the  
UKAEA  
Publications Officer, Culham Science Centre, Building K1/0/83 Abingdon, Oxfordshire,  
OX14 3DB, UK. The United Kingdom Atomic Energy Authority is the copyright holder.

# **On a fusion born triton effect in JET deuterium discharges with H-minority ICRF heating**

Vasili Kiptily, F. Belli, J. Eriksson, C. Hellesen, V. Goloborod'ko,  
K. Schöpf



# On fusion born triton effects in discharges with H-minority ICRF heating of JET deuterium plasmas

V.G. Kiptily<sup>1</sup>, F Belli<sup>2</sup>, J. Eriksson<sup>3</sup>, C. Hellesen<sup>3</sup> and JET contributors <sup>a</sup>

<sup>1</sup> Culham Centre for Fusion Energy, UKAEA, Culham Science Centre, Abingdon, OX14 3DB, UK

<sup>2</sup> Unità Tecnica Fusione, ENEA C. R. Frascati, via E. Fermi 45, 00044 Frascati (Roma), Italy

<sup>3</sup> Department of Physics and Astronomy, Uppsala University, SE-75120 Uppsala, Sweden

<sup>a</sup> See author list [X. Litaudon et al 2017 Nucl. Fusion 57 102001]

E-mail: [vasili.kiptily@ukaea.uk](mailto:vasili.kiptily@ukaea.uk)

## Abstract

An effect due to fusion born triton production has been observed in JET high-performance deuterium plasma discharges with NBI and H-minority ICRF heating, using DD and DT neutron spectrometry as well as fusion product loss measurements. The observations show that increase of the triton burn up rate leads to decrease of second harmonic  $\omega_{cH} = 2\omega_{cD}$  enhancement of DD neutron rate and an acceleration of tritons due to absorbing ICRH power at the third harmonic  $\omega = 3\omega_{cT}$ . This effect indicates a redistribution of ICRH power absorption at  $\omega \approx \omega_{cH} = 2\omega_{cD} = 3\omega_{cT}$  towards increase of triton concentration at the ion cyclotron resonance layer. It determines the necessity to consider the ICRH power absorption  $\omega = 3\omega_{cT}$  in modelling of high-performance deuterium discharges with simultaneous NBI and H-minority ICRF heating for development of DT plasma scenarios and fusion rate predictions.

---

In addition to the deuterium neutral beam injection (NBI), heating of deuterium plasmas with waves in the ion cyclotron range of frequencies (ICRF) is exploited to develop high-performance scenarios (H-mode, hybrid and advanced) in the preparation of forthcoming Joint European Torus (JET) deuterium tritium (DT) experiments. In our case, in the hybrid scenario discharges with plasma current  $I_p = 2.2$  MA and central toroidal field  $B_T(0) = 2.8$ T, a combined deuterium NBI and hydrogen-minority ICRF heating  $\omega \approx \omega_{cH} = 2\omega_{cD} = 3\omega_{cT}$  at  $f = \omega/(2\pi) \approx 42.5$  MHz of dipole phasing is used. Applying ICRH, power damping at  $\omega = \omega_{cH}$  dominates, neutron rate increases due to  $\omega = 2\omega_{cD}$  damping by D-ions and the plasma performance is enhanced. As rule, ICRH power damping at  $\omega = 3\omega_{cT}$  is neglected. Here, we will show that ignorance of the  $\omega = 3\omega_{cT}$  damping by fusion born tritons is not justified in high-performance discharges.

In the deuterium plasmas, neutrons are produced due to the fusion reaction  $D + D = n$  (2.45 MeV) +  $^3\text{He}$  (0.82 MeV). With a roughly the same probability, the second branch of

this fusion,  $D + D = p$  (3.02 MeV) +  $t$  (1.01 MeV) gives rise to tritons. These tritons “burnup” during slowing down generating 14-MeV neutrons due to the reaction  $D + T = {}^4\text{He}$  (3.6 MeV) +  $n$  (14.1 MeV) with a maximum of the emission at resonance  $E_T \approx 160$  keV in the cross-section. Previously, triton burnup measurements have been carried out on different tokamaks [1-6] studying confinement and slowing-down of fast tritons in deuterium plasmas. The DT neutron emission can reach up to 3% of total neutron rate in JET high-performance deuterium discharges.

In this Letter, we report on experimentally observed variations in DD and DT neutron spectra as well as fusion product losses which correlated with rate of the fusion born triton production in JET high-performance deuterium plasma discharges with NBI and H-minority ICRF heating.

Measuring neutrons by means of the time-of-flight spectrometer TOFOR [7] in the high-performance JET discharges, we observed some changes in DD neutron spectra, which are correlated towards increase of the triton burnup rate, i.e. 14-MeV neutron rate. It was selected several similar hybrid discharges #92393, 92394, 92395 and 92398 characterised by a quiet and stable plasmas in two specific time periods, which were chosen for the analysis. As an example, waveforms of the discharge #92394 are shown in figure 1. We defined the time slot 46.25s – 47.25s as a period of the low average triton burnup rate (LTB) and the time slot 47.25s – 47.85s as a period of the high average triton burnup rate (HTB). One can see that in the LTB period, neutron rate is growing up at a stable ICRH power. The slowing down parameter  $\tau_e \sim T_e^{3/2}/n_e$  [8], where  $T_e$  and  $n_e$  are the electrons temperature and density, grows with some saturation at the end. Note, the triton burnup rate and the delay of 14-MeV neutron emission relative to total neutron rate depend on this parameter. Triton losses measured with fast ion loss detector (FILD) [9] follow to the neutron rate that indicates a classical type of fusion product loss. The HTB period is characterised by quite steady parameters with very small increase of neutron rate. This time slot was chosen in such a way as to avoid the unstable fishbone period of strong triton losses with typical spikes seen.

The figure 2 demonstrates why we selected these time slots as LTB and HTB rate periods. You can see waveforms of the total neutron rate together with relative 14-MeV neutron and 17-MeV  $\gamma$ -ray rates, which are associated with DT fusion rate. We used NE213 detector based on a liquid scintillator with a tangential line-of-sight [10] for 14-MeV neutron measurements. This is a broadband neutron spectrometer of MeV energy-range, which allows recording DD and DT neutron spectra. Gamma-rays related to triton burnup are produced in

the reaction  $D + T = {}^5\text{He} + \gamma$  (16.84 MeV), which is a weak branch ( $\sim 10^{-4}$ ) of the main DT fusion reaction giving rise to 14-MeV neutrons. These  $\gamma$ -rays were measured with bismuth-germanite detector (BGO), which is viewing the plasma in the tangential line-of-sight [11]. In the figure you can see that maximums of both 14-MeV neutrons and 17-MeV gammas are a bit shifted due to slowing down of tritons and increase of their density.

It was found that the TOFOR spectra recorded in LTB and HTB are rather different in all selected high-performance discharges. Indeed, in the discharge #92394 (figure 3), you can see that number of neutrons detected with time of flight in the range  $t_{TOF} = 45 - 55$  ns is much higher in the LTB rate period than in HTB one. We need to note that the time of flight varies inversely with neutron velocity and energy:  $t_{TOF} \sim \frac{1}{v_n} \sim \frac{1}{\sqrt{E_n}}$ , and this  $t_{TOF}$  range is related to DD neutron energies  $E_n \approx 3.5 - 5.1$  MeV. The measured TOFOR spectra could be partitioned on components due to thermonuclear (TH), beam-thermal (NBI), ICRF heating induced (RF) and scattered neutrons [8, 12]. Such spectrum partitioning is shown in figure 3, where one can see that RF neutrons in LTB period are more energetic than those in HTB period. It is also can be seen in figure 4 that shows the fitted TOFOR neutron spectra presented as counts vs neutron energies  $E_n$  in the LTB and HTB rate periods.

According to kinematics of the  $D(D, n){}^3\text{He}$  reaction, energy of neutrons depends on the energy of reacted deuterons. In our case, energy of ICRF accelerated deuterons is much higher than the bulk ion temperature,  $E_D \gg T_D$ , and  $E_n = 2.45 \text{ MeV} + 0.5E_D + 0.5\sqrt{3E_D(3.27 \text{ MeV} + 0.5E_D)} \cos \theta_n$ , where  $\theta_n$  is an angle between neutron and deuterium velocities in the lab system. So, neutrons detected in the energy range  $E_n \approx 3.5 - 5.1$  MeV were produced by deuterons in the energy range  $E_D \approx 0.25 - 1.35$  MeV. Since the NBI deuterium energies were below 125 keV, such energetic neutrons appeared in spectra due to the ICRF acceleration of D-ions at  $\omega \approx \omega_{cH} = 2\omega_{cD}$ , and thus in average  $\bar{E}_D^{LTB} > \bar{E}_D^{HTB}$ .

We observed the similar distinctive feature of TOFOR spectra in all selected discharges. The sums of the spectra in both chosen periods are presented in figure 5. It is important to note that by contrast to spectrum in figure 5(a) recorded in LTB periods, a peak at  $t_{TOF} \approx 27$  ns, which is related to 14-MeV neutrons due to triton burnup in the HTB period, is clearly seen in figure 5(b).

For analysis of the ICRH neutron enhancement we used the ratio  $I_{RF}/(I_{TH} + I_{NBI})$  obtained from the least-square fitting procedure of spectrum components shown in figure 3.

As an example, the ICRH neutron enhancement factors have been calculated and presented in figure 6 together with waveforms of total neutron, DT neutron and 17-MeV  $\gamma$ -ray rates. One can see that during the HTB periods this factor drops dramatically. Hence, this is an additional confirmation that the decrease of the second harmonic  $\omega_{cH} = 2\omega_{cD}$  deuteron acceleration results in the reduction of intensity of energetic neutrons, when density of fusion born tritons increased.

Measurements with NE213 detector allowed us to confirm the TOFOR results and to study the triton burnup directly, analysing both DD and DT neutron spectra. Neutron detection with NE213 detector based on elastic scattering of neutrons by light nuclei (ordinary hydrogen) in the scintillator. This is a recoil/proton-recoil detector. Neutron transfer a portion on kinetic energy  $E_n$  to nucleus mass  $A$  (recoil nucleus/proton)  $E_R = \frac{4A}{(1+A)^2} E_n (\cos \theta_n)^2$ . The recoil nucleus/proton losses its energy  $E_R$  in the scintillator. So, the recoil energies are distributed continuously between of zero and maximum of possible,  $E_n$  in the case of mass  $A = 1$ ; in our case it is related to  $E_n^{DD} \approx 2.5$  MeV and  $E_n^{DT} \approx 14.1$  MeV. A sum of normalised neutron spectra recorded with NE213 spectrometer in the high-performance discharges ## 92393, 92394, 92395 and 92398, which are the same as have been used for the TOFOR data analysis, presented in figure 7. The summation was done in both LTB and HTB periods. It is clearly seen an intensive DD peak and DT neutrons with 14-MeV edge in the recoil spectra. A zoom of the high-energy tail of the DD part of the neutron recoil spectra is shown in figure 8. One can see that the NE213 data confirms the TOFOR results, i.e. neutrons in LTB period are more energetic than in the HTB one and thus  $\overline{E}_D^{LTB} > \overline{E}_D^{HTB}$ .

Neutron recoil spectra related to DT-neutrons are shown in figure 9. For the analysis of this low statistics data, we used a fitting of the logistic function  $F(x) = \frac{A}{1+e^{k(x-x_0)}}$ . Normalised fitted logistic curves related to the LTB and HTB rate periods are presented in figure 10(a). In the 1<sup>st</sup> approximation, the derivatives of the logistic function shown in figure 10(b) could characterise the 14-MeV neutron emission spectra due to triton burnup. One can see that DT neutron recoil spectra obtained in such a way carry some features, which are opposite to DD neutron spectra in chosen time slots. Indeed, the HTB spectrum is broader (~10%) than LTB one. Taking into account kinematics of the reaction  $T + D = {}^4\text{He} + n(14.1 \text{ MeV})$  in the case of  $E_T \gg T_D$ , which gives dependence  $E_n = 14.1 \text{ MeV} + 0.44E_T + 0.62\sqrt{E_T(17.6 \text{ MeV} + 0.4E_T)} \cos \theta_n$ , we can conclude that tritons upon average are more

energetic in the HTB period,  $\overline{E}_T^{HTB} \approx 1.2 \overline{E}_T^{LTB}$ . Hence, this effect indicates an acceleration of tritons by absorbing ICRH power at  $\omega = 3\omega_{cT}$  due to a redistribution of ICRH power absorption towards increase of triton concentration at the ion cyclotron resonance layer.

A correlation of triton losses measured by FILD with rate of the fusion born triton production was observed as well. A typical footprint of ion losses recorded by FILD in the discharge #92394 is presented in figure 11. Striking the scintillator plate, both lost fusion tritons ( $\approx 1$  MeV) and protons ( $\approx 3$  MeV) induce light collected with CCD camera. However, light emission produced by tritons in the thin scintillator layer is dominates ( $\sim 90\%$ ) because protons are too energetic to stop in it.

We compared the gyro-radius distributions of lost tritons in both LTB and HTB periods integrating the highest light output (dash line in figure 11) in the pitch-angle range  $55^\circ - 58^\circ$ , which is relevant to the FILD instrumental width. The smoothed and normalised gyro-radius distributions in figure 12(a) show that light emission recorded in the HTB rate period is shifted to high gyro-radii relative to the LTB one. In this discharge the triton energy is related to gyro-radius as  $E_T(\text{MeV}) \approx 0.1 + 0.075 \rho(\text{cm})^2$ , so the lost triton energy distributions look like it depicted in figure 12(b). One can see that tritons lost in the period of the HTB rate is more energetic, thus FILD data confirms the results of the DT neutron measurements with NE213-detector, i.e.  $\overline{E}_T^{HTB} > \overline{E}_T^{LTB}$ .

Summarising the results obtained in the selected high-performance discharges with NBI and H-minority ICRF heating, we ascertained following:

- DD neutron measurements with TOFOR show that the average deuteron energies  $\overline{E}_D^{LTB} > \overline{E}_D^{HTB}$
- The ICRF neutron enhancement factor due to  $\omega = 2\omega_{cD}$  is decreasing in the HTB rate period towards the increase of triton burnup rate and triton density growing up in vicinity of the IC resonance layer.
- DD neutron measurements with NE213-detector confirm the TOFOR data.
- DT neutron measurements with NE213-detector show that spectrum related to the HTB rate period is broader than spectrum related to the LTB one and the average triton energies  $\overline{E}_T^{HTB} > \overline{E}_T^{LTB}$ . A balance between slowing down and acceleration of tritons due to  $\omega \approx \omega_{cH} = 2\omega_{cD} = 3\omega_{cT}$  ICRF power absorption is only credible explanation of this effect.

- Gyro-radius/energy distributions of lost tritons measured with FILD consistent with DT neutron measurements indicating that the average triton energies

$$\overline{E}_T^{HTB} > \overline{E}_T^{LTB} .$$

In conclusion, presented in the Letter effects demonstrate a measurable redistribution of ICRF power absorption at  $\omega \approx \omega_{cH} = 2\omega_{cD} = 3\omega_{cT}$  and an acceleration of tritons due to absorbing ICRF power at  $\omega = 3\omega_{cT}$  towards increase of triton concentration at the IC resonance layer. Hence, developing high performance deuterium plasma scenarios with NBI and H-minority ICRF heating for application in DT experiments, the 3<sup>rd</sup> harmonic triton damping of ICRH should be considered. Also, we can emphasise that triton burnup measurements in high performance deuterium plasma discharges can help in validation of auxiliary ICRF plasma heating models and optimisation of plasma scenarios.

### **Acknowledgements**

We are grateful to C. Challis, S. Sharapov, K. McClements, H. Weisen, Ye. Kazakov, D. Van Eester and M. Mantsinen for fruitful discussions. This work has been carried out within the framework of the EUROfusion Consortium and has received funding from the Euratom research and training programme 2014-2018 under grant agreement No 633053 and from the RCUK Energy Programme [grant No EP/P012450/1]. To obtain further information on the data and models underlying this paper please contact [PublicationsManager@ukaea.uk](mailto:PublicationsManager@ukaea.uk) . The views and opinions expressed herein do not necessarily reflect those of the European Commission.

## References

- [1] Heidbrink W. W., Chrien R.E. and Strachan J. D., 1983 *Nucl. Fusion* **23** 917
- [2] Källne J. *et al* 1988 *Nucl. Fusion* **28** 1291
- [3] Conroy S. *et al* 1988 *Nucl. Fusion* **28** 2127
- [4] Strachan J.D. *et al* 1996 *Nucl. Fusion* **36** 1189
- [5] Nishitani T. *et al* 1996 *Plasma Phys. Control. Fusion* **38** 355
- [6] Ballabio L. *et al* 2000 *Nucl. Fusion* **40** 21
- [7] Stitzer L. Jr, *Physics of Fully Ionized Gases*, Interscience, New York (1962)
- [8] Gatu Johnson M. *et al* 2008 *Nucl. Instrum. Methods Phys. Res. A* **591** 417
- [9] Darrow D. *et al* 2006 *Rev. Sci. Instrum.* **77** 10E701
- [10] Belli F. *et al* 2012 *IEEE Trans. Nucl. Science* **59** 2512-19
- [11] Kiptily V. *et al* 2002 *Nucl. Fusion* **22** 999-1007
- [12] Hellesen C. *et al* 2010 *Nucl. Fusion* **50** 022001

## Figure captions

Figure 1. Waveforms of the discharge #92394. Grey vertical lines denote time slots: 46.25s – 47.25s is the low average triton burnup rate (LTB) and 47.25s – 47.85s is the high average triton burnup rate (HTB).

Figure 2. Waveforms of total neutron rate (solid line), DT-neutron rate detected with NE213 spectrometer (filled circles) and  $\gamma$ -ray rate in the energy window 12 -17 MeV detected with bismuth-germanite (BGO) detector (open circles).

Figure 3. DD-neutron spectra recorded with time-of-flight spectrometer TOFOR (dots): (a) the spectrum was recorded during the LTB rate period; (b) the spectrum was recorded during the HTB rate period. Lines are the fitted components of the spectra related to thermal (TH) and NBI beam – target neutrons (BT), neutrons due to ICRF D-ion acceleration at  $\omega = 2\omega_{cD}$  (RF), backscattered neutrons (scatt).

Figure 4. A comparison of neutron spectra recorded by TOFOR during the LTB and HTB rate periods.

Figure 5. A sum of DD-neutron spectra recorded with time-of-flight spectrometer TOFOR in similar high-performance discharges ## 92393, 92394, 92395 and 92398: (a) the spectrum is related to the LTB rate periods; (b) the spectrum is related to the HTB rate periods.

Figure 6. Waveforms of the high-performance discharge #92398 as shown in figure 3. Grey rectangles denotes the changes of the ICRH enhancement factor inferred from the TOFOR data.

Figure 7. A sum of normalised neutron spectra recorded with NE213 spectrometer in similar high-performance discharges ## 92393, 92394, 92395 and 92398; blue - spectrum recorded during the LTB rate period; red – spectrum recorded during the HTB rate period.

Figure 8. A part of the neutron spectra shown in figure 7, which is related to the high energy tail of DD-neutrons.

Figure 9. A part of the neutron spectra shown in figure 7, which is related to DT-neutrons: (a) the spectrum is related to the LTB rate period; (b) the spectrum is related to the HTB rate period; solid line – a fitted logistic curve (see text).

Figure 10. Normalised logistic curves (a) shown in figure 9 and their derivatives (b) related to the LTB (blue) and HTB (red) rate periods.

Figure 11. A footprint of ion losses in the discharge #92394 obtained with FILD: red solid line – a position of the IC resonance on the gyro-radius vs pitch-angle grid; dash red line – a pitch-angle related to maximal light emission produced by lost fusion tritons and protons.

Figure 12. Smoothed gyro-radius (a) and energy (b) distributions of lost tritons related to the maximal FILD light emission (dash line in figure 11); the distributions are averaged over the pitch-angle instrumental width  $\sim 55^\circ - 58^\circ$ .

**Figures**

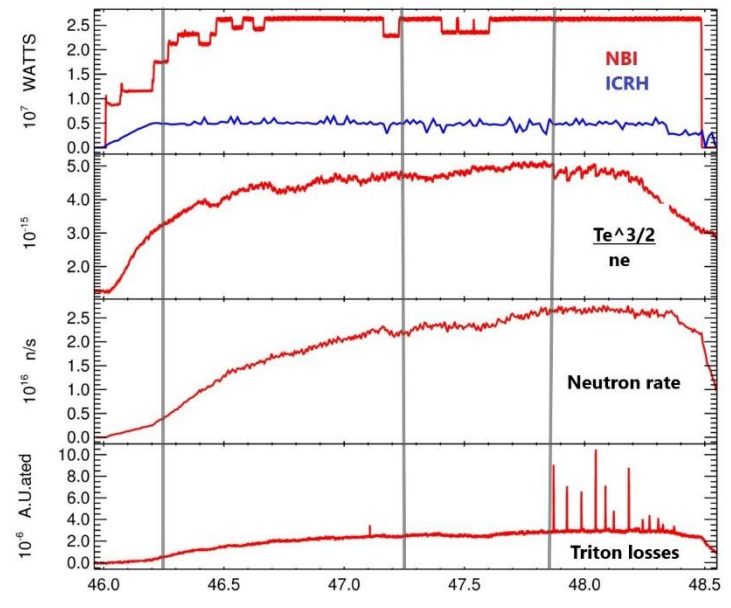


Figure 1.

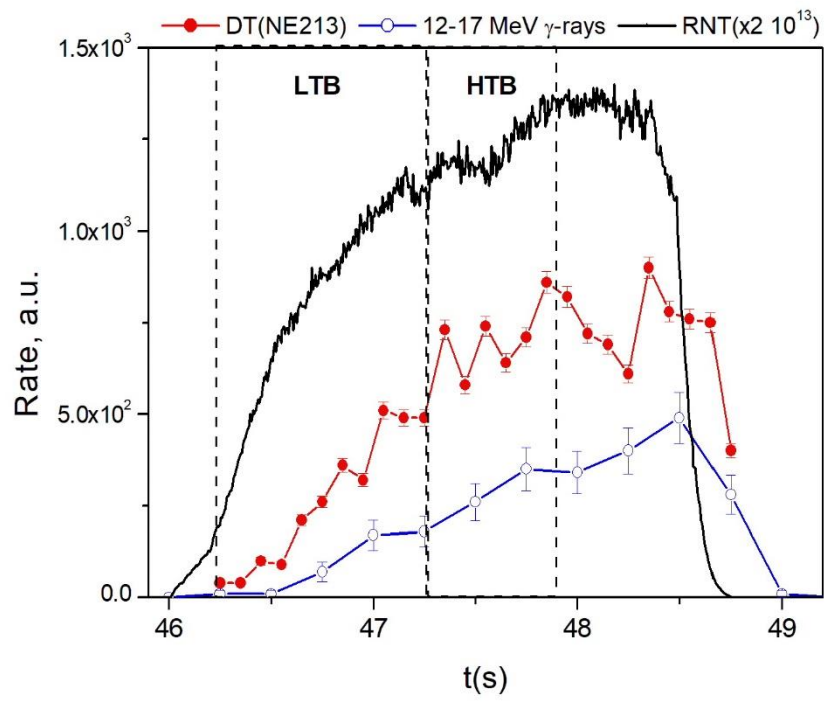


Figure 2.

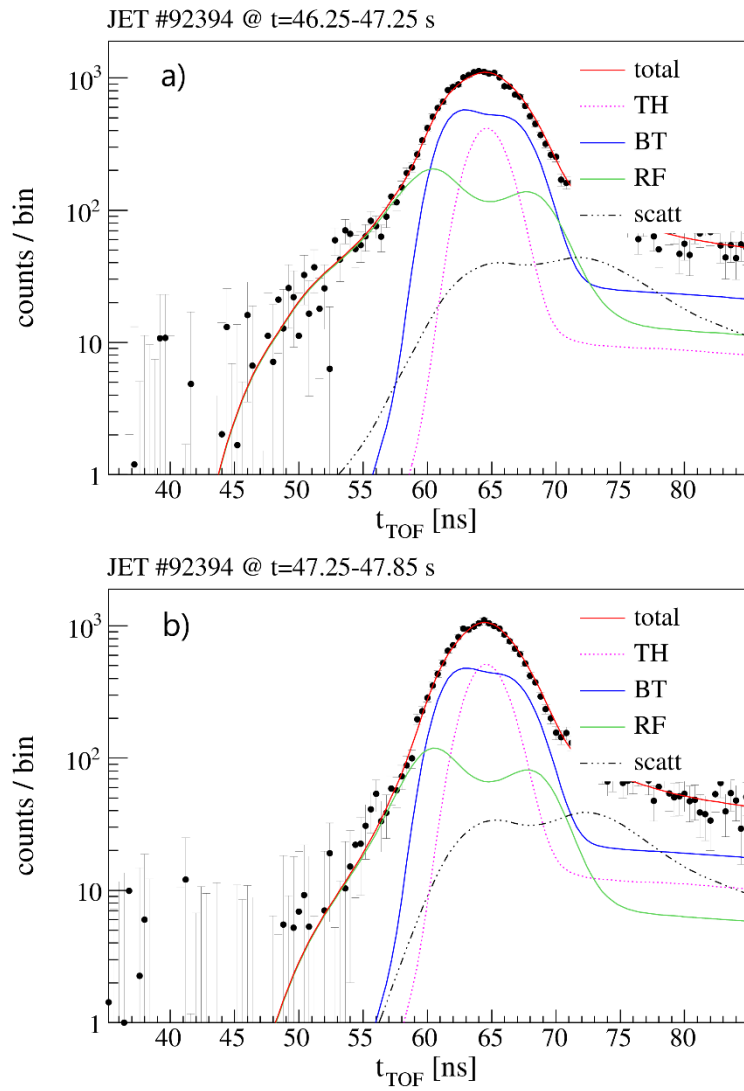


Figure 3.

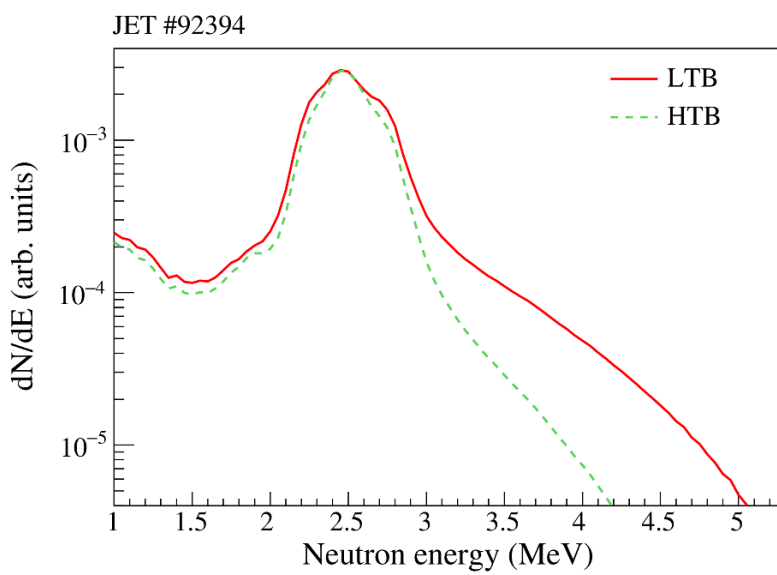


Figure 4.

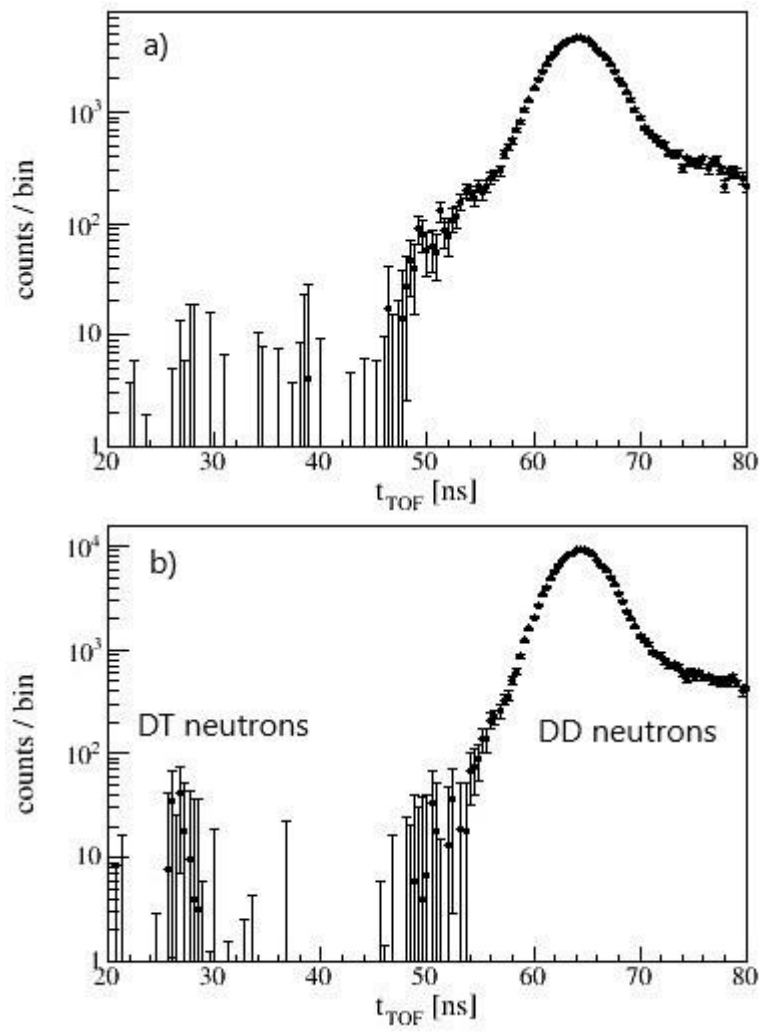


Figure 5.

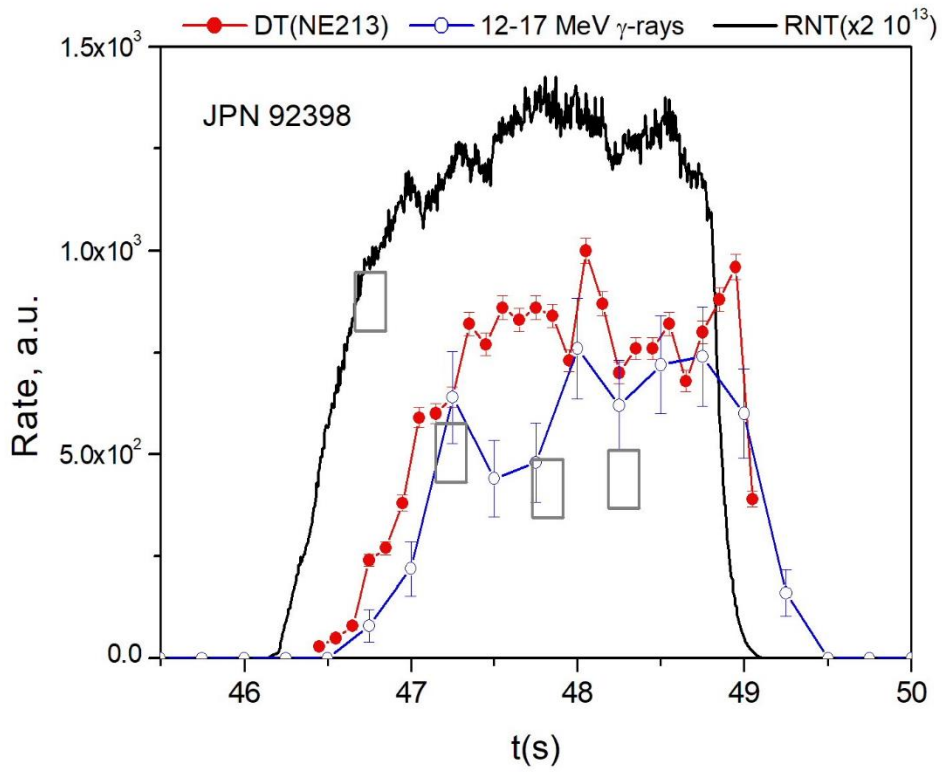


Figure 6.

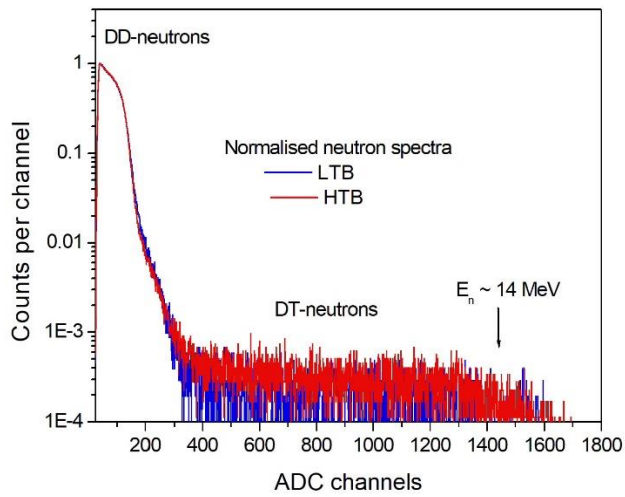


Figure 7.

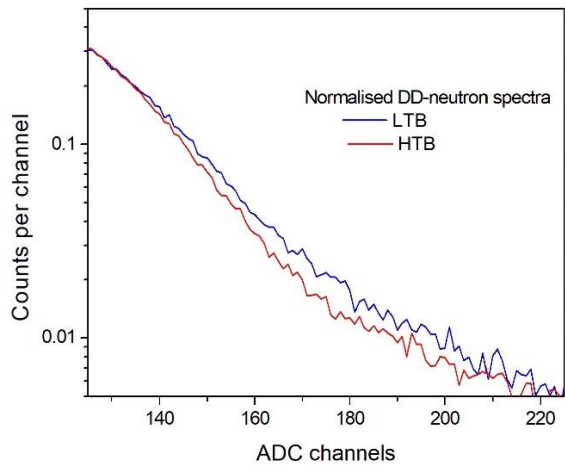


Figure 8.

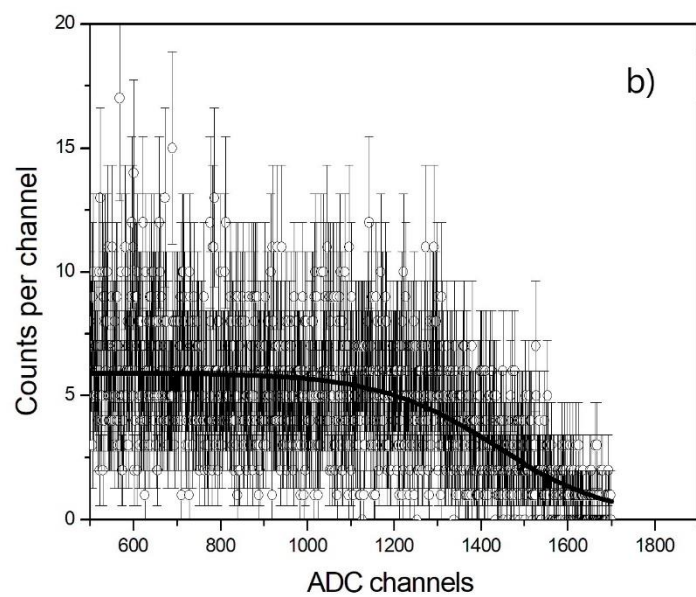
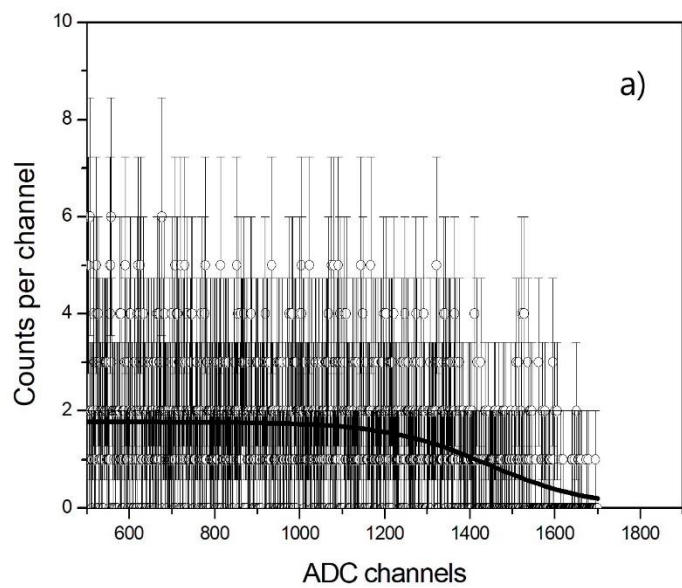


Figure 9.

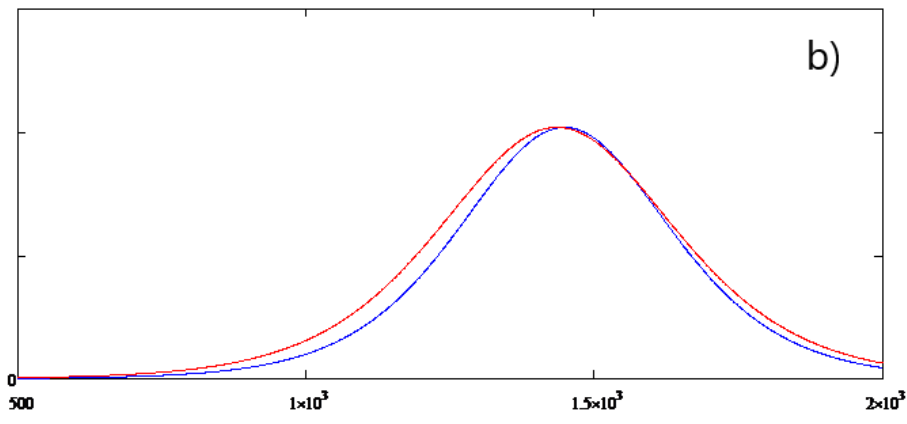
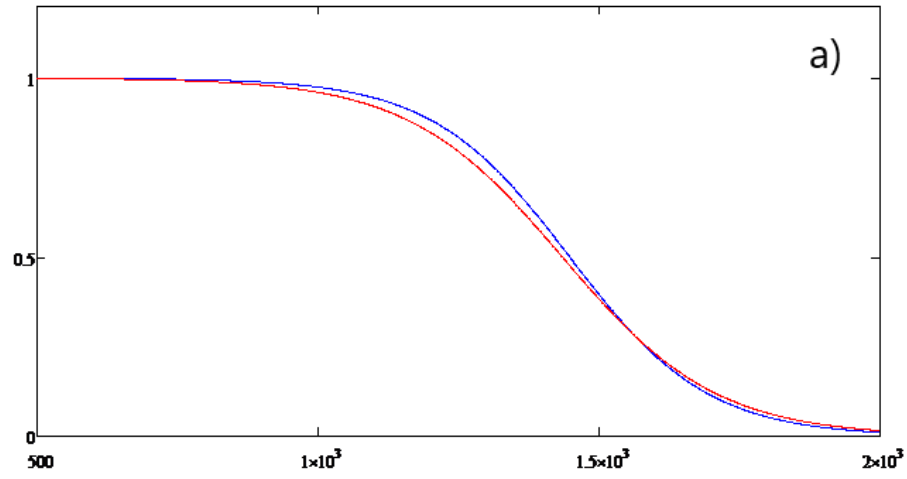


Figure 10.

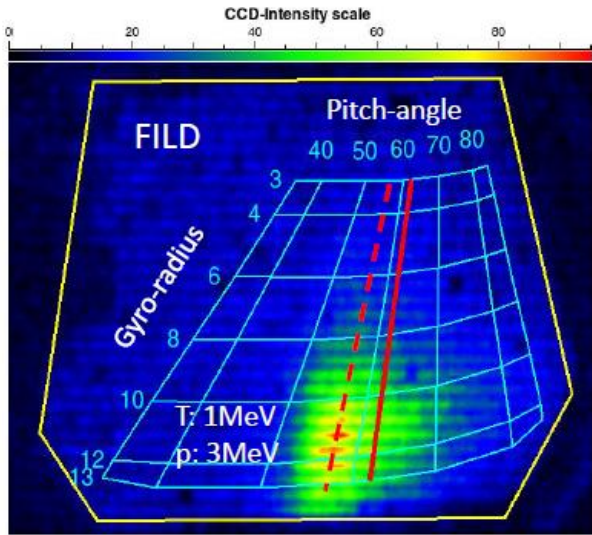


Figure 11.

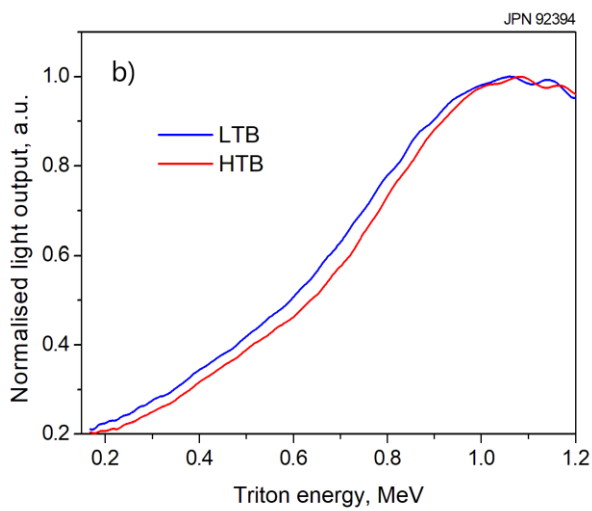
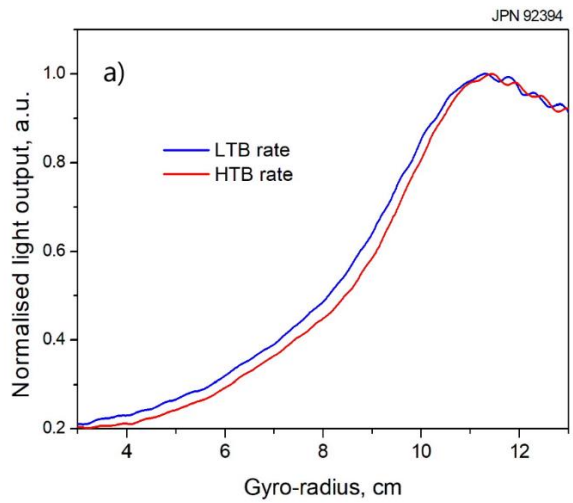


Figure 12.